Bio-inspired gold microtubes based on morphology of filamentous fungi.

Journal:	*Biomaterials Science*
Manuscript ID:	BM-COM-01-2014-000030
Article Type:	Communication
Date Submitted by the Author:	27-Jan-2014
Complete List of Authors:	Fontes, Adriana; Universidade Federal da Bahia, Physical Chemistry Geris, Regina; Universidade Federal da Bahia, Organic Chemistry Santos, Arnaud; Universidade do Estado da Bahia, DCET -Campus I Pereira, Madson; Universidade do Estado da Bahia, DCET Ramalho, Jéssica; Universidade Federal da Bahia, Campus de Ondina, Instituto de Física da Silva, Antonio; Universidade Federal da Bahia, Campus de Ondina, Instituto de Física Malta, Marcos; Universidade Federal da Bahia, Physical-Chemistry

SCHOLARONE™
Manuscripts

Journal Name

Biomaterials Science

Dynamic Article Links ▶

ARTICLE TYPE

Bio-inspired gold microtubes based on morphology of filamentous fungi

Adriana M. Fontes,[a] **Regina Geris,**[a] **Arnaud V. dos Santos,**[b] **Madson G. Pereira,**[b] **Jéssica G. S. Ramalho,**[c] **Antonio F. da Silva**[c] **and Marcos Malta***[a]

This communication describes a general method for templating fungal filaments with gold nanoparticles that results in a gold replica of filaments after calcination of the
10 **biological template.**

During the last 500 million years, Nature has developed a multitude of structures and chemical building blocks (biomolecules) with precise control of function/architecture,
15 which was essential for the survival of living organisms in practically all environments on Earth.[1] By using a few chemical elements such as C, H, O, N, P, S, Si and Ca, in mild conditions of temperature and pH, biological systems can form complex structures, which are hierarchically organised at the nano, micro,
20 meso and macroscales.[2] Excellent examples include the multifunctional siliceous skeletons of diatoms and radiolarians, the ordered microstructure based on chitin of butterfly wings or the arrangement of microcrystals of hydroxyapatite with protocollagen that form the bones of mammals.[3]
25 Classical synthetic routes (precipitation, sol-gel, solvothermal, etc.) are very limited to produce materials with complex forms due to the lack of specific interactions between the basic building blocks. In this way, scientists have been seeking inspiration from Nature through the use of microorganisms as biotemplates to
30 produce hybrid inorganic/biological structures with optimised properties. For instance, Belcher *et al.* produced a hybrid system constituted by the CoO_3/M13 virus and applied it as a cathode for high-energy lithium ion batteries with an improved specific capacity and rate capability.[4] In recent years, the cultivation of
35 filamentous fungi in media containing noble metal nanoparticles (NPs) has resulted in the formation of tubular filaments covered with a metallic layer that, in fact, could be used as catalysts or as microwires for electric applications and sensing.[5-8]
In this communication, we describe the production of a large
40 aspect ratio, spatially controlled, three-dimensional gold microtubes (Au-μTs), obtained through the calcination of self-assembled Au nanoparticles (Au-NPs) deposited onto filamentous fungi. We have found that optimising the ratio of citrate/Au-NPs, there is an improvement in the assembly of Au-NPs on the cell
45 wall of microorganisms, which led to special tube-like structures after critical point drying and removal by calcination of the fungal biotemplate (Scheme 1). This methodology provides a convenient way to obtain metallic microstructures in the scale of

cellular entities, in which they could perform specific functions as
50 microcapsules, high surface area electrodes, catalyst support, metallic Y junction, electroactive channels, substrates for SERS analysis and so on.[9] To the best of our knowledge, this is the first time that template-free microtubular Au structures, which replicates fungi morphologies have been obtained using these
55 microorganisms as scaffolds.
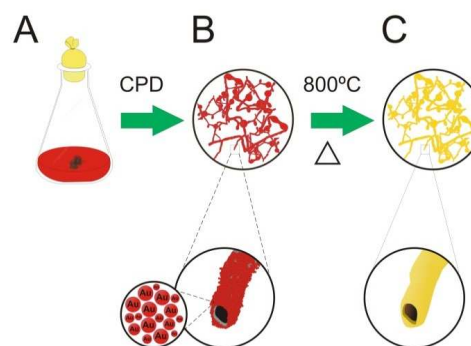
Scheme 1: Illustration of the formation of Au-μTs. (a) Fungi are cultivated in citrate-stabilised Au-NPs medium for two months. (b) Bio-hybrid material is harvested and dried using critical point drying (CPD) to preserve tubular morphology.
60 **(c) Calcination of bio-hybrid fungus/Au-NPs at 800 °C produces Au-μTs.**

Our work originated from previous conjectures about the feasibility to produce metal microtubes (i.e., tubular replica of the
65 fungal filaments with diameters of 1–5 micrometers) using bio-hybrid fungi/Au-NPs as the starting material.[6, 7] In a former study conducted by Hussain and co-workers, porous Au microwires were produced through the thermal elimination of biological templates of the hybrid *Aspergillus niger*/Au-NPs.[10] However,
70 the formation of the microtubes and details of the architecture of the microorganism were not observed. In fact, two major challenges related to the homogeneity of the metal layer in the microbial cell wall and the maintenance of the tubular morphology of the hybrid material must be considered. First, due
75 to microbiological characteristics, fungal species have a variable "affinity" for noble metals.[11] It is, therefore, mandatory to choose those fungi that grow in media poor in nutrients (usually containing only citrate or glutamate) as well as with a large

capacity to acquire NPs. Second, microorganisms are cultivated in liquid medium and thus, air drying leads to the collapse of the biological structure due to the effects of surface tension. Therefore, point critical drying or lyophilisation is necessary to
5 preserve the delicate microtubular fungus/NP shape.

Based on methodology proposed by Eychmuller *et al.*,[7] we hypothesise that by selecting fungal species with a large affinity to Au-NPs and optimising conditions for mycelia growth, it would be possible to enhance the assembly of Au-NPs at the
10 fungal cell wall. Therefore, by careful drying of the samples using CPD, the elimination of the biotemplate could be conducted by a simple calcination step, which retains the morphology of microorganisms and produces metal microtubes.

To prove this concept, solutions of Au-NPs with variable
15 molar ratios between citrate and gold ([Cit]:[Au^{3+}] = 0.3, 2.0, 3.7, 7.1 and 17.3) were prepared in order to verify the optimal conditions for Au deposition above four biological templates: *Phialomyces macrosporus*, *Trichoderma* sp., *Penicillium* sp. and *Aspergillus niger*. These fungi were carefully chosen from a set
20 of previous experiments done in our laboratories, which used selected species with higher affinity to metal NPs. As a result of the triple role of the citrate ions in this synthesis, i.e., carbon source for the microorganisms, buffering agent and electrostatic stabilising for NPs, solutions of Au-NPs were investigated with
25 respect to their stability using UV-vis spectrophotometry (see ESI Fig. S1). Despite variable amounts of citrate ions in each sample, all colloidal solutions were stable for months and any signal of gold coagulation/precipitation was observed (ESI, Fig. S2). Nevertheless, if we compare the optical properties of fresh Au-
30 NPs solutions with aged samples, a slight change in the visible spectra is observed, indicating aggregation of NPs to some extent.[12]

Analyses of energy-dispersive X-rays (EDX) were performed in order to provide a quick evaluation of the affinity of these
35 fungal species to the noble metals. Initially, it was reasoned that solutions with lower citrate concentrations ([Cit]:[Au^{3+}] = 0.3 and 2.0), would improve the enrichment of NPs onto fungal biotemplates, due to the consumption of citrate and subsequent destabilisation of Au-NPs.[13] However, EDX data of the bio-
40 hybrids showed that this assumption was observed only for *Trichoderma* sp., in which other specimens presented an erratic trend in the accumulation of Au-NP (ESI, Fig. S3).

To gain insight about the spatial distribution of self-organised Au-NPs on mycelial tissue, thin-section transmission electron
45 microscopy analyses (TEM) were performed. Figure 2 (a) represents the cross-sectioned undecorated *P. macrosporus* showing a typical fungal ultrastructure. Low magnification TEM [Figure 2(b)] revealed that the bio-hybrid presents cell integrity, with cytoplasmic structures not being affected by NPs. The
50 deposition of Au-NPs occurs exclusively onto the fungal cell wall, assembling a circumference with a thickness of ≈ 0.8 μm in the region studied. The NPs with ≈ 17 nm and nearly spherical shapes are relatively separated from each other [Figure 2 (c) and (f)], leading to the occurrence of some fungi/Au-NP
55 superstructures with a reddish colour, similar to the Au colloidal solution. TEM imaging of a longitudinal cross-sectioned isolated hyphae, Figure 2 (d)–(f), revealed an ideal assembly of Au-NPs, which decorated homogeneously all extension of the tubular cell.
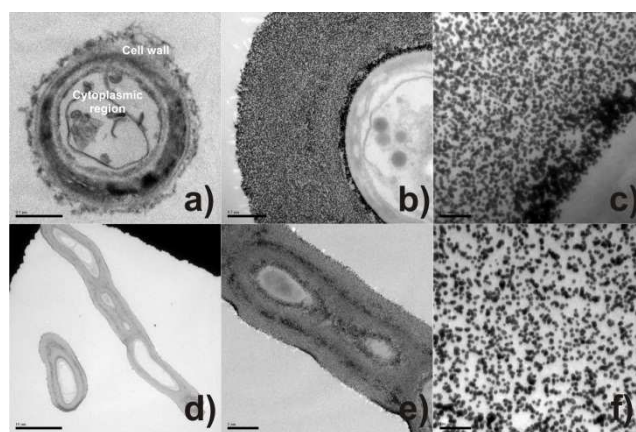
Figure 2: TEM micrographs of the transversal cross-
60 sectioned region of undecorated *P. macrosporus* (a) and bio-hybrid *P. macrosporus* growth in a solution [Cit]:[Au^{3+}] = 3.7 at (b) 50,000X and (c) 100,000X magnifications. TEM micrographs of longitudinal cross-sectioned bio-hybrid *P. macrosporus* growth in a solution [Cit]:[Au^{3+}] = 2.0 at (d)
65 3,000X (e) 10,000X and (f) 200,000X magnifications.

At present, the process of self-assembly of metal NPs onto filamentous fungi remains unclear due to the chemical complexity of the hyphae wall added to the little understanding
70 regarding interaction forces between microorganisms and Au-NPs. Attempts to elucidate the assembly of Au-NPs onto the fungal cell wall of *P. macrosporus* (studied as a model organism) were carried out by using TEM (Figure 3). In these micrographs the biological components are not apparent since specimens were
75 not post-fixed with osmium tetroxide, providing information uniquely about the arrangement of Au-NPs. Figure 3 (a) and (c) shows the morphological characterisation of Au-NPs when the molar ratios of [Cit]:[Au^{3+}] were 0.3 and 2.0. Spaced nanoparticles of around 15 nm are accumulated on the tubular
80 hyphae with any signal of aggregation (see Figure 3 (b) for details). As a characteristic of these hybrid materials, a thick layer of NPs (≈ 1.0 μm) decorating the microorganisms are observable in TEM images. In contrast, dramatic changes occur in the assembly of NPs at higher citrate concentrations ([Cit]:[Au^{3+}] =
85 3.7, 7.1 and 17.3). Particularly, images d), e) and f) of Figure 3 show Au-NPs more aggregated at the biotemplate, forming a compact layer with a large broad size distribution of nanoparticles.

It is quite surprising that citrate stabilised nanoparticles still
90 privileged binding to negatively charged surfaces of the microorganisms forming a robust metallic layer.[8, 14] Although we do not fully understand this apparent inconsistency, we suspect that there are two regimes for the assembling of Au-NPs governed by ionic strength of the NPs solutions (see ESI Table
95 S1). Initially, in solutions with lower citrate concentrations, the growing of fungus provokes an exhaustion of these ions near to the cell wall causing an electrical de-stabilisation of Au-NPs.[15] Due to weak interaction between citrate and Au-NPs, it is reasonable to suppose that components of cell wall (amino acids residues and
100 polysaccharides chains based on 1,3-ß-glucan) could dislocate the remained citrate ions, binding directly on the surface of NPs.[16] In this proposal, Au-NPs would be sterically stabilised by the

microfibrilar biopolymers of the cell wall during physiological processes. Therefore, while spaced Au-NPs are assembled on the cell wall, more nanoparticles could diffuses from the bulk to the vicinity of microorganism, decorating the fungal hyphae in subsequent layers.

In constrast, hybrid *P. macrosporus*/Au-NPs cultivated in solutions at higher citrate concentrations presents a dense metallic layer, with interconnected Au-NPs heavily loaded around microorganisms (Figure 3 (d), (e) and (f)). At these circumstances, the increase of ionic strength causes a reduction in the thickness of the electric double layer of the Au-NPs, decreasing the interparticle electrostatic repulsion which usually is accompanied by de-stabilisation of the NPs. Au-NPs are, eventually, closer each other, which leads only a partial stabilisation of NPs by components of cell wall. Therefore, during fungal growth in solutions with higher ionic strength, the metallic component is assembling forming agglomerates entrapped in the constituents of the cell wall. These findings can be important for future application of these hybrids materials in areas such as catalysis where the size, shape and the assembling of NPs are important parameters in the efficiency of the catalyst.
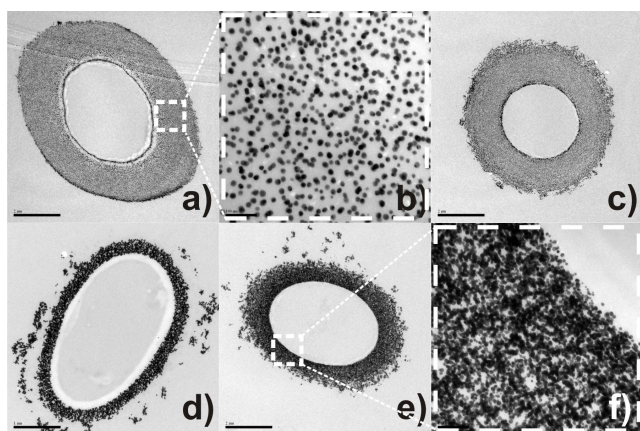
Figure 3: TEM micrographs of the transversal cross-sectioned bio-hybrid *P. macrosporus*/Au-NPs cultivated in solutions [Cit]:[Au^{3+}] = (a-b) 0.3, (c) 2.0, (d) 7.1 and (e-f) 17.3.

A scanning electron micrograph of hybrid *P. macrosporus*/Au-NPs obtained in backscattering mode, showed uniformity of the mycelial mass with individual hyphae covered with a dense layer of Au-NPs [Figure 4 (a)]. Globose chlamydospores (GC, see arrow) were observed in two fungal cultures, namely *P. macrosporus* and *Trichoderma* sp. These terminal or intercalary hyphae structures are resistant spores, which survive in unfavourable environmental conditions, and their production can be the result of the medium used in our study, which exhibits a low content of nutrients. *P. macrosporus* hypha diameter varies from 2–8 µm and up to several millimetres in length (ESI, Fig. S4). Bio-hybrid superstructure presented X-ray diffraction pattern (XRD), Figure 4(b), characteristics of Au fcc (PDF 04-0784) illustrating the crystallinity of the primary Au-NPs. Figure 4 (c) shows comparative thermogravimetric analyses (TG) of the undecorated *P. macrosporus* and *P. macrosporus*/Au-NPs at a flow rate of 50 mL.min^{-1} of synthetic air. Approximately 2 mg of the materials was placed in a Pt crucible, and the investigations were carried out at a constant heating rate of 10 ^{o}C.min^{-1} in the temperature range of 25–800 ^{o}C. Mass losses for both samples, associated with the burn of the biological template were recorded up to about 600 °C, and no further mass loss was observed up to 800 °C. Undecorated *P. macrosporus* showed two exothermic mass losses at 325 ^{o}C and 495 ^{o}C. The presence of Au-NPs in the *P. macrosporus* modified the TG profile, which showed lower temperatures of decomposition, i.e., 310 and 391 ^{o}C, indicating that the presence of metal accelerated the elimination of the organic components. After thermogravimetric experiments, a gold piece was obtained and no further treatment was carried out to SEM studies.

The reaction product of *P. macrosporus*/Au-NPs, consisted almost exclusively of gold in massive form (with a small fraction of ashes), with an interconnected fibrilar structure and diameters varying from 1.5–2.5 µm [Figure 4(d)]. The structure of the Au-µTs significantly contracted when compared with the original bio-hybrids, probably due to volatilisation of the components of cell wall, which leads to shrinking of the metal microstructure. Despite SEM images resembling fungal morphology, naked-eye visualisation of this material is similar to the gold bulk [see ESI Fig. S5].
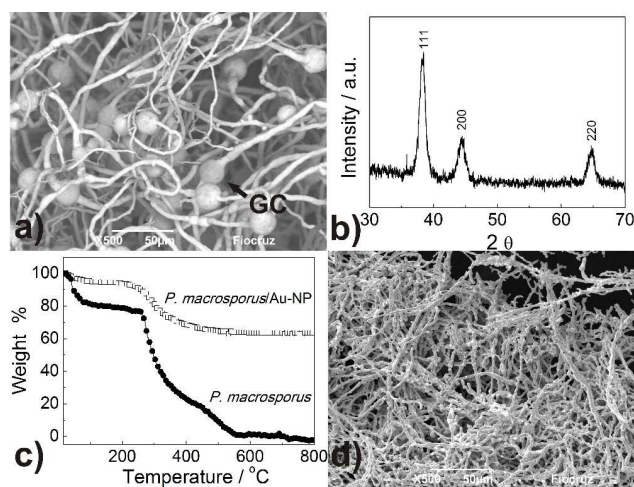
Figure 4: (a) SEM micrograph and (b) DRX analysis of *P. macrosporus*/Au-NPs after critical point drying; (c) thermogravimetric analysis of undecorated *P. macrosporus* and *P. macrosporus*/Au-NPs after critical point drying; (d) SEM micrograph of Au-µTs obtained from calcination of *P. macrosporus*/Au-NPs. All experiments refer to the bio-hybrid growth in a solution [Cit]:[Au^{3+}] = 7.1.

For this synthesis, there is an important influence of the type of biotemplate and the concentration of the citrate ions, which provides the possibility to control the tube morphology to some extent. For instance, *P. macrosporus*/Au-NPs cultivated in solutions of [Cit]:[Au^{3+}] = 7.1 (in our experiments the best conditions for the deposition of NPs in this microorganism), produce Au-µTs with thicker walls and irregular surface morphology (see ESI Figures S5 and S6 for other examples). Figure 5 shows the calcined microtubular replicas of *Trichoderma* sp/Au-NPs (a-b), *Aspergillus niger*/Au-NPs (c-d) and *Penicillium* sp/Au-NPs (e-f) with a smooth, thin wall thickness that nearly mimics the morphologies of the biotemplates. In Figure 5 (a), it is possible to visualise a tube

opening (with diameter ≈1.0 μm) and a sphere that resembles globose chlamydospore (GC) while in (b), an isolated Au-μT developed a morphology of a segmented hyphae. Finally, thin-section TEM analyses of a calcined *Trichoderma* sp/Au-NPs's replica revealed the aggregation of individual NPs to produce bulk gold and confirm the preservation of the tubular characteristics of the microorganisms (ESI, Fig. S7).
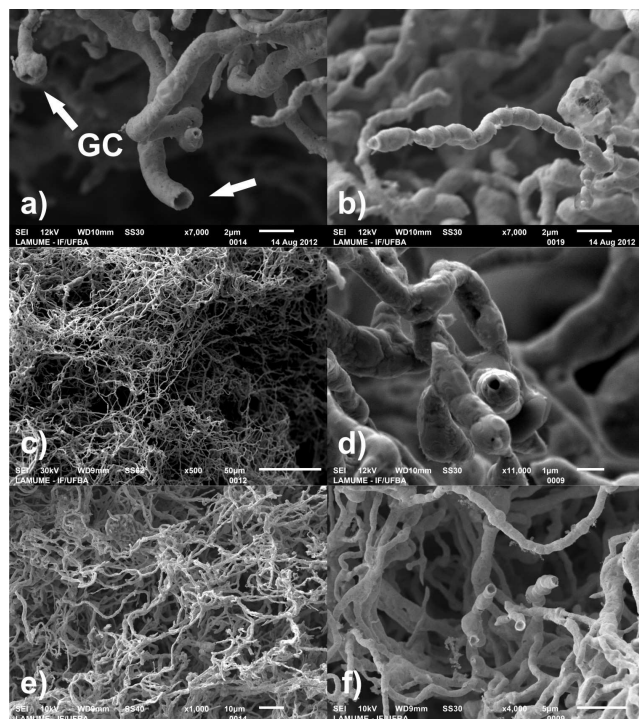
Figure 5: SEM micrographs of Au-μTs (fungi replica) obtained from *Trichoderma* sp/Au-NPs (a-b), *Aspergillus niger*/Au-NPs (c-d) and *Penicillium* sp/Au-NPs (e-f). All products refer to the calcined bio-hybrids growth in solution [Cit]:[Au^{3+}] = 0.3.

In conclusion, we report a general method to synthesise microtubular Au structures (which mimics morphology of microorganisms) through self-assembly of Au-NP about filamentous fungi and subsequent elimination of the biological template by simple calcination. Three significant aspects must be observed to obtain these materials: (i) it is important to choose microorganisms with higher affinity to Au-NPs and viable to growth in a medium poor in nutrients; (ii) the ionic strength of solutions affect the assembly of NPs over microorganisms and its control have an important role in the final shape of metallic replica; (iii) critical point drying (or another method of dehydration) is essential to avoid agglomeration of NPs in the cell wall and destruction of the tubular morphology of the biotemplate. Further studies to understand the interactions between NPs and cell walls, the use of other noble metals (such as platinum and palladium) to produce such microtubes and the application of Au-μTs as high surface area electrodes are currently underway in our laboratories.

Notes and references

ᵃ Instituto de Química, Universidade Federal da Bahia, Campus Ondina, Salvador (BA), Brazil. Fax: 55 71 3237 4117; Tel: 55 71 3283 6850; E-mail: marcosmalta@ufba.br
ᵇ Departamento de Ciências Exatas e da Terra, Universidade do Estado da Bahia, Salvador (BA), Brazil. Fax: 55 71 3117 2277; Tel: 55 71 3117 2283;
ᶜ Instituto de Física, Universidade Federal da Bahia, Campus Ondina, Salvador (BA), Brazil. Fax: 55 71 3283 6606; Tel: 55 71 3283 6616;

† Electronic Supplementary Information (ESI) available: See DOI: 10.1039/b000000x/

1 C. Sanchez, H. Arribart and M. M. G. Guille, *Nature Materials*, 2005, **4**, 277.
2 L. B. Liu, X. R. Duan, H. B. Liu, S. Wang and Y. L. Li, *Chemical Communications*, 2008, 5999.
3 J. P. Vernon, Y. N. Fang, Y. Cai and K. H. Sandhage, *Angewandte Chemie-International Edition*, 2010, **49**, 7765; S. Mann and G. A. Ozin, *Nature*, 1996, **382**, 313; R. Lakes, *Nature*, 1993, **361**, 511; C. Mille, E. C. Tyrode and R. W. Corkery, *Chemical Communications*, 2011, **47**, 9873.
4 K. T. Nam, D. W. Kim, P. J. Yoo, C. Y. Chiang, N. Meethong, P. T. Hammond, Y. M. Chiang and A. M. Belcher, *Science*, 2006, **312**, 885.
5 Z. Li, S. W. Chung, J. M. Nam, D. S. Ginger and C. A. Mirkin, *Angewandte Chemie-International Edition*, 2003, **42**, 2306.
6 A. Sugunan, P. Melin, J. Schnurer, J. G. Hilborn and J. Dutta, *Advanced Materials*, 2007, **19**, 77.
7 N. C. Bigall, M. Reitzig, W. Naumann, P. Simon, K. H. van Pee and A. Eychmuller, *Angewandte Chemie-International Edition*, 2008, **47**, 7876.
8 R. F. Fakhrullin, A. I. Zamaleeva, R. T. Minullina, S. A. Konnova and V. N. Paunov, *Chemical Society Reviews*, 2012, **41**, 4189.
9 X. J. Huang, A. M. O'Mahony and R. G. Compton, *Small*, 2009, **5**, 776; J. Ye, J. D. Jiang, Y. S. Zhao and J. N. Yao, *Journal of Materials Chemistry*, 2012, **22**, 19202; T. Wang, R. Zheng, X. Hu, L. Zhang and S. Dong, *Journal of Physical Chemistry B*, 2006, **110**, 14179; J. J. Gooding, R. Wibowo, J. Q. Liu, W. R. Yang, D. Losic, S. Orbons, F. J. Mearns, J. G. Shapter and D. B. Hibbert, *Journal of the American Chemical Society*, 2003, **125**, 9006.
10 A. Rehman, M. I. Majeed, A. Ihsan, S. Z. Hussain, R. Saif ur, M. A. Ghauri, Z. M. Khalid and I. Hussain, *Journal of Nanoparticle Research*, 2011, **13**, 6747.
11 N. C. Bigall, A. K. Herrmann, M. Vogel, M. Rose, P. Simon, W. Carrillo-Cabrera, D. Dorfs, S. Kaskel, N. Gaponik and A. Eychmuller, *Angewandte Chemie-International Edition*, 2009, **48**, 9731.
12 S. Mandal, A. Gole, N. Lala, R. Gonnade, V. Ganvir and M. Sastry, *Langmuir*, 2001, **17**, 6262.
13 A. Sabah, I. Dakua, P. Kumar, W. S. Mohammed and J. Dutta, *Digest Journal of Nanomaterials and Biostructures*, 2012, **7**, 583.
14 S. Sharma and S. Srivastava, *Biosensors & Bioelectronics*, 2013, **50**, 174.
15 A. Sabah, P. Kumar, W. S. Mohammed and J. Dutta, *Particle & Particle Systems Characterization*, 2013, **30**, 473.
16 S. H. Brewer, W. R. Glomm, M. C. Johnson, M. K. Knag and S. Franzen, *Langmuir*, 2005, **21**, 9303; X. W. Jia, X. J. Xu and L. N. Zhang, *Biomacromolecules*, 2013, **14**, 1787.